

GaN Monolithic Power Amplifiers for Microwave Backhaul Applications

Original

GaN Monolithic Power Amplifiers for Microwave Backhaul Applications / Quaglia, R., Camarchia, V., Pirola, M., Ghione, G.. - In: ELECTRONICS. - ISSN 2079-9292. - ELETTRONICO. - 5:2(2016), pp. 1-12. [10.3390/electronics5020025]

Availability:

This version is available at: 11583/2643229 since: 2017-05-31T15:58:21Z

Publisher:

MDPI AG (Basel, Switzerland)

Published

DOI:10.3390/electronics5020025

Terms of use:

This article is made available under terms and conditions as specified in the corresponding bibliographic description in the repository

Publisher copyright

(Article begins on next page)

Article

GaN Monolithic Power Amplifiers for Microwave Backhaul Applications

Roberto Quaglia ¹, Vittorio Camarchia ^{2,*}, Marco Pirola ² and Giovanni Ghione ²

¹ Centre for High Frequency Engineering, Cardiff University, CF103AT Cardiff, Wales, UK; quagliar@cardiff.ac.uk

² DET, Politecnico di Torino, Corso Duca degli Abruzzi, 24, 10129 Torino, Italy; marco.pirola@polito.it (M.P.); giovanni.ghione@polito.it (G.G.)

* Correspondence: vittorio.camarchia@polito.it; Tel.: +39-011-0904219

Academic Editor: Farid Medjdoub

Received: 10 March 2016; Accepted: 25 May 2016; Published: 1 June 2016

Abstract: Gallium nitride integrated technology is very promising not only for wireless applications at mobile frequencies (below 6 GHz) but also for network backhaul radiolink deployment, now under deep revision for the incoming 5G generation of mobile communications. This contribution presents three linear power amplifiers realized on 0.25 μm Gallium Nitride on Silicon Carbide monolithic integrated circuits for microwave backhaul applications: two combined power amplifiers working in the backhaul band around 7 GHz, and a more challenging third one working in the higher 15 GHz band. Architectures and main design steps are described, highlighting the pros and cons of Gallium Nitride with respect to the reference technology which, for these applications, is represented by gallium arsenide.

Keywords: Gallium Nitride; MMIC; power amplifiers; microwave backhaul

1. Introduction

The constantly growing demand of high data rates of today's communication systems drives us towards the adoption of high spectral efficient digital modulation schemes posing severe channel linearity constraints on all the transceiver building blocks. This is particularly true for Power Amplifiers (PAs) in the transmitter chain [1,2]. The classical solution of recovering linearity by back-off of the amplifier degrades the efficiency, another key aspect of PAs. At frequencies below 6 GHz, powerful linearizers can be adopted to recover linearity, because the additional power consumption is a fraction of the total power involved. Instead, for microwave backhaul, where power levels do not exceed dozens of Watts, the adoption of complex linearizers with high impact on the overall power budget is not always feasible, thus making the linearity of the PA alone very important [3]. For these cases, to keep the PA linearity at an acceptable level, the solution of choice is the class AB PA, that represents a reasonable trade-off between linearity, efficiency and bandwidth [2].

Regarding the technology, in parallel to the reference choice of gallium arsenide (GaAs), which is cheap, mature and available from many suppliers, Gallium Nitride (GaN) integrated technology is attracting a lot of interest at research level, especially for power applications, thanks to its superior characteristics in comparison to GaAs [4–6], mainly in terms of power density. Focusing on PAs, this technology leads to lower size and better power dissipation (when using SiC substrate), favourable input and output matching impedances, all features positively affecting overall losses, and eventually efficiency [7].

Moreover, the possibility of integrating the transistor and the matching networks in a single Microwave Monolithic Integrated Circuit (MMIC) PA is of crucial importance to minimize weight and component count, and to improve repeatability and reliability of the microwave front-ends. GaN on

SiC MMIC processes have been developed and can practically make use of the same passive structures used for GaAs MMICs, that have reached a good technological maturity.

This work presents the design, characterization, and linearization of three class AB PA examples designed for microwave backhaul applications adopting the 0.25 μm GaN HEMT on SiC Qorvo Monolithic Microwave Integrated Circuits (MMIC) technology. The first two MMICs have been designed in the backhaul band around 7 GHz, while the third PA is one of the first examples of the possible exploitation of the commercial 0.25 μm GaN HEMT on SiC technology also in the 15 GHz band.

The paper is organized as follows: Section 2 presents design strategies, C.W. experimental characterization and system level characterization of the 7 GHz MMICs. In Section 3 the same approach is extended to the description of the 15 GHz PA. Finally, in Section 4, some conclusions are drawn.

2. Combined Class AB PAs for 7 GHz Microwave Backhaul

The first two PA examples have been designed and fabricated for the microwave backhaul band around 7 GHz, with a target output power of 5 W in a 10% band. The focus of the design was on keeping the amplitude to phase conversion as low as possible (below 10 degrees). This has a crucial impact on the linearity of the PA, while maximizing the back-off efficiency. To this aim, two different strategies have been followed regarding the harmonic termination of the active device, as will be described in next section.

2.1. Design Strategy and Fabrication

The adopted MMIC process is the 0.25 μm GaN HEMT on SiC of Qorvo (formerly Triquint Semiconductor) [8]. Considering the device power density of 4.5 W/mm for 30 V drain bias of the process and accounting for the network losses, two $8 \times 75 \mu\text{m}$ GaN HEMTs have been combined with a resulting total periphery of 1.2 mm.

For the two designs only the effects of fundamental and 2nd harmonic loads have been considered, realizing two similar stages only differing for second harmonic control of the output termination. In the first case (the Tuned Load amplifier), the 2nd harmonic voltage is nulled at the intrinsic drain, making the output combiner resonant and limiting the bandwidth (see a detailed schematic in Figure 1). In the second example (the Harmonic Tuned amplifier), the 2nd harmonic is optimized to maximize the efficiency (detailed schematic in Figure 2). In this case, the load is non-resonant with clear advantages in terms of bandwidth. On the other hand, the latter approach presents some degrees of risk because it is strongly based on the non-linear model accuracy. In particular, second harmonic manipulation can negatively affect PA linearity with effects that can only be evaluated and corrected relying on a large signal model. For this reason, extensive simulations have to be performed to analyze the possible impact of the second harmonic load on AM/AM and AM/PM curves, also accounting for a possible inaccuracy of the large signal model by statistically varying its most sensitive parameters. More details on this approach can be found in [9].

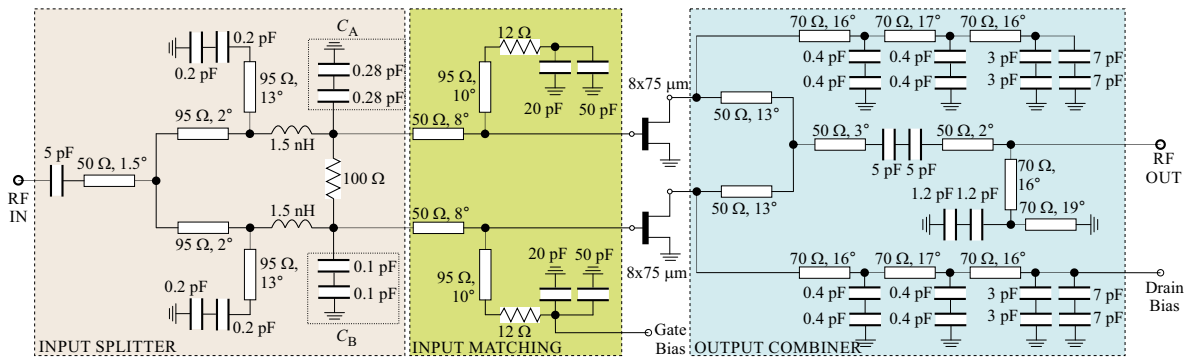


Figure 1. Complete scheme of the Tuned Load Amplifier. Equivalent ideal lines are represented: electrical length refers to 7 GHz.

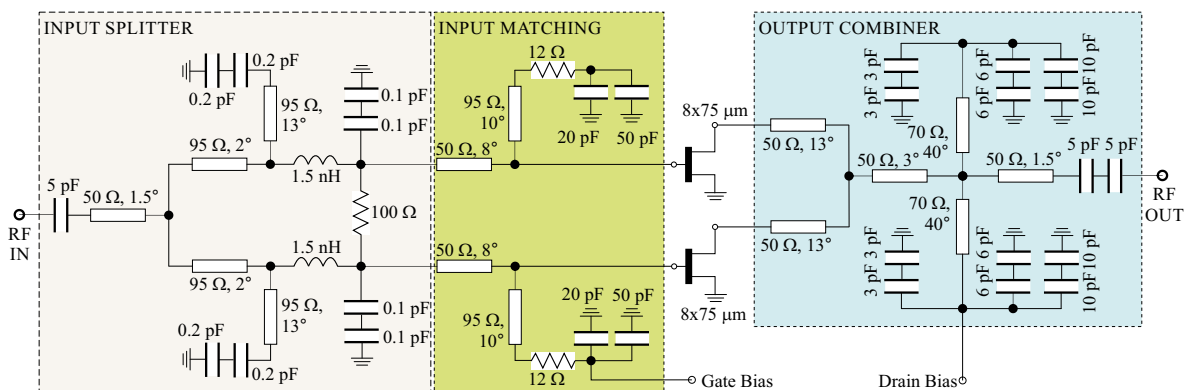


Figure 2. Complete scheme of the Harmonic Tuned amplifier. Equivalent ideal lines are represented: electrical length refers to 7 GHz.

The same load at the fundamental frequency has been adopted for both stages. It has been chosen according to a classical design approach based on load-pull simulations across the amplifier bandwidth to extract a simplified output equivalent circuit of the device [10–12], eventually adopted for the synthesis of the output matching network.

The real part of the load is 125 Ω, while the reactive part can be modeled on the the whole design band with a 0.18 pF capacitance. Notice that, in the case of the 2nd harmonic control, the chosen fundamental load can be increased, since the “overshoot” of the fundamental component of voltage is compensated by the 2nd harmonic component (see [13]).

Figure 3 show the synthesized loads at fundamental and 2nd harmonic around 7 GHz for the Tuned Load PA Figure 3a (in a 10% bandwidth), and Harmonic Tuned PA Figure 3b (in a 20% bandwidth).

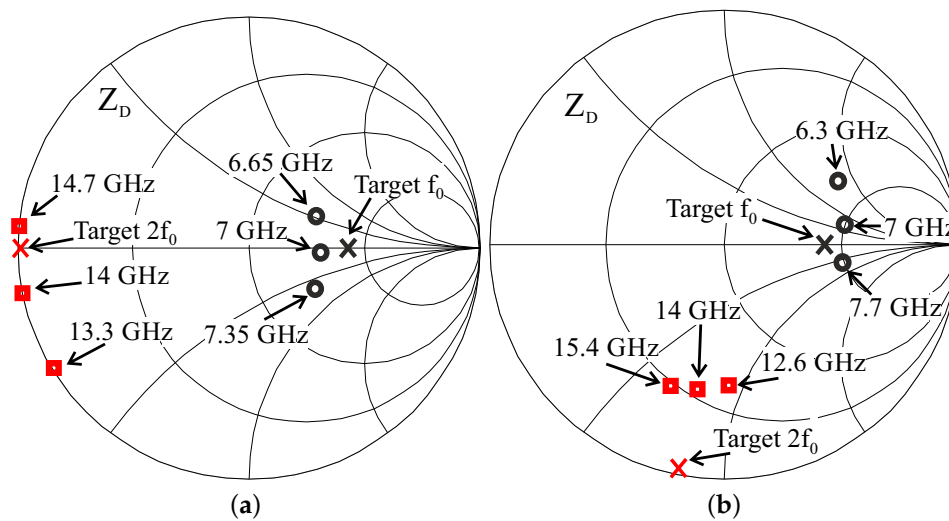


Figure 3. Optimum fundamental (black cross) and second harmonic (red cross) loads for the $8 \times 75 \mu\text{m}$ device, for Tuned Load (a) and Harmonic Tuned (b) designs. Synthesized loads at fundamental (black circles) and correspondent second harmonic (red squares) in a 10% bandwidth for the Tuned Load case, and in a 20% bandwidth for the Harmonic Tuned case.

The input section, common in both stages, includes a Wilkinson input power splitter and a matching network from the device gate to 50Ω , ensuring at the same time broadband unconditional stability, thanks to a 12Ω series resistor, and gate bias feeding. Loop analysis has been performed to verify the stability of the PAs. A semi-lumped strategy assuring good matching, bandwidth and robustness to process variations has been adopted. Out-of-band spurious oscillations have been prevented by adding small asymmetries in the input splitter capacitors without affecting significantly the in-band behaviour and performance.

The Tuned Load and Harmonic Tuned MMICs are shown in Figure 4a,b, respectively. The chip size of the modules are $2.8 \times 1.9 \text{ mm}^2$ and $2.8 \times 2.8 \text{ mm}^2$, respectively.

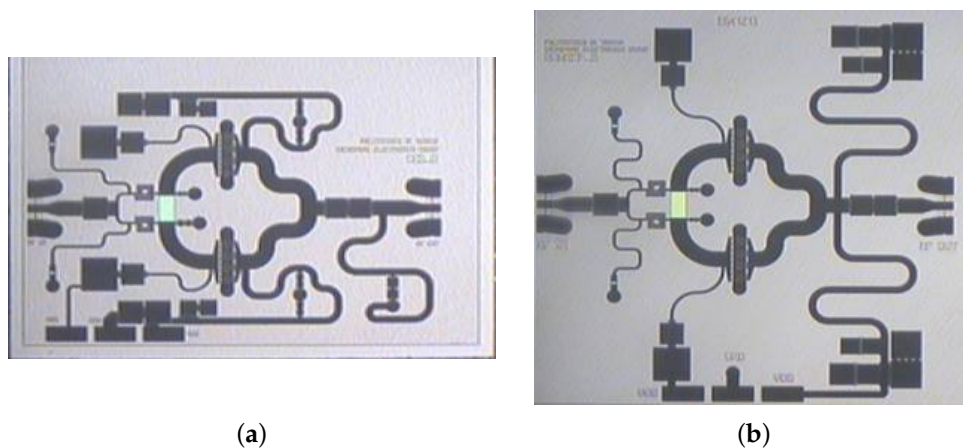


Figure 4. Microscope picture of the Tuned Load ($2.8 \times 1.9 \text{ mm}^2$) (a), and Harmonic Tuned ($2.8 \times 2.8 \text{ mm}^2$) (b) Microwave Monolithic Integrated Circuit (MMIC) amplifiers.

2.2. Experimental Characterization

The MMICs have been characterized in small signal in the band 4–12 GHz, and in large signal in a 30% band around 7 GHz. Linearity has been assessed through system level characterization adopting

a 256-QAM, 7 MHz channel modulated input signal [14]. The drain bias voltage adopted for CW and modulated analysis is 30 V for both PAs. The drain bias current is 60 mA and 30 mA for Tuned Load and Harmonic Tuned stage, respectively.

2.2.1. Continuous Wave

Figure 5a,b shows the simulated and measured scattering parameters for the Tuned Load and the Harmonic Tuned stages, respectively. The Tuned Load stage bandwidth limitation, due to the resonant nature of the employed output matching, can be observed.

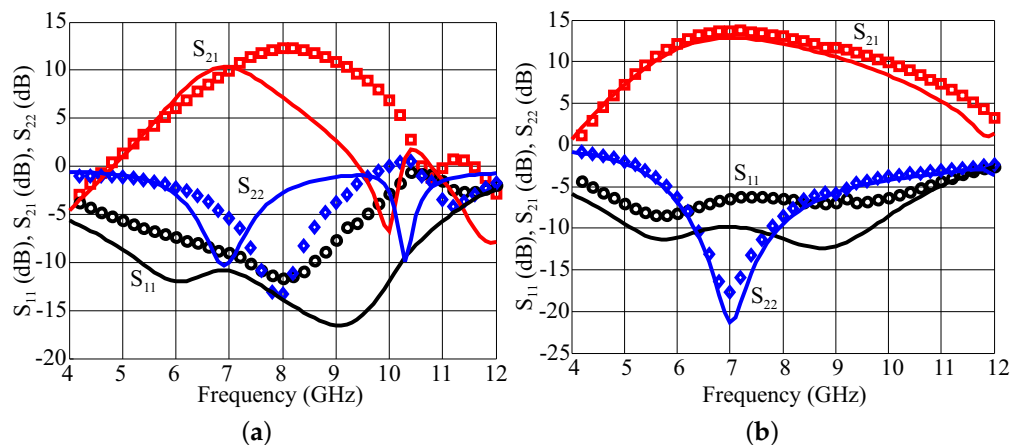


Figure 5. Scattering parameters in the band 4–12 GHz. Tuned Load (a), Harmonic Tuned (b) Power Amplifiers (PAs). Simulations: solid lines; measurements: symbols. S_{11} : black circles, S_{21} : red squares, S_{22} : blue diamonds.

Single tone characterization results, compared with simulations, are reported in Figure 6a,b. The saturated output power is of 35.6 dBm and 36.6 dBm, with a corresponding efficiency of 33% and 50%, and a small signal gain of 10.7 dB and 12 dB for the Tuned Load and Harmonic Tuned PA, respectively.

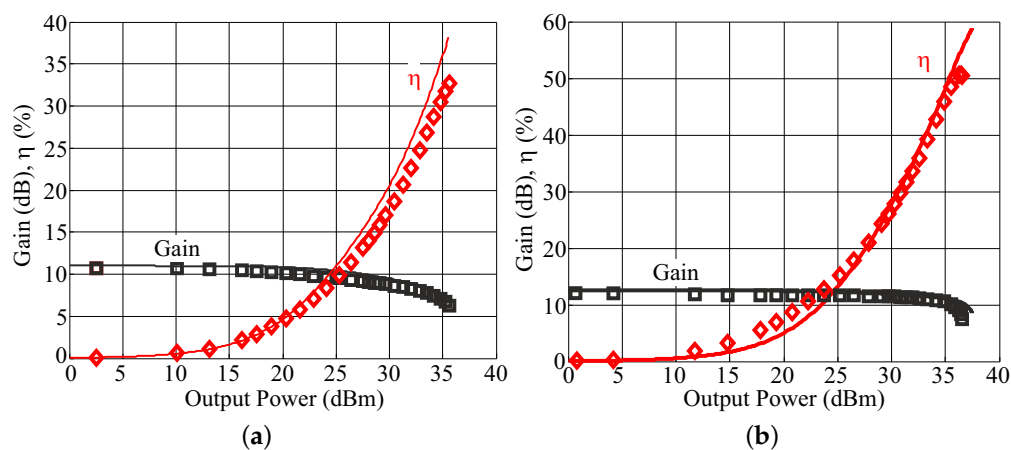


Figure 6. Measured power sweeps at 7 GHz of the Tuned Load (a) and Harmonic Tuned (b) PAs. Drain bias voltage is 30 V for both PAs. Drain bias current is 60 mA and 30 mA respectively. Simulations: solid lines; measurements: symbols. Gain: black squares, efficiency: red diamonds.

Figure 7a,b show the Continuous Wave performance *vs.* frequency of both MMICs. Regarding the Tuned Load PA, the saturated output power results are higher than 35 dBm in the 6.7–7.9 GHz band, while the saturated efficiency is higher than 35% in the 7.2–7.6 GHz band. On the other hand, the

Harmonic Tuned PA exhibits an output power in excess of 36 dBm from 6.4 to 8.3 GHz, with saturated efficiency higher than 50% in the 7–7.8 GHz range.

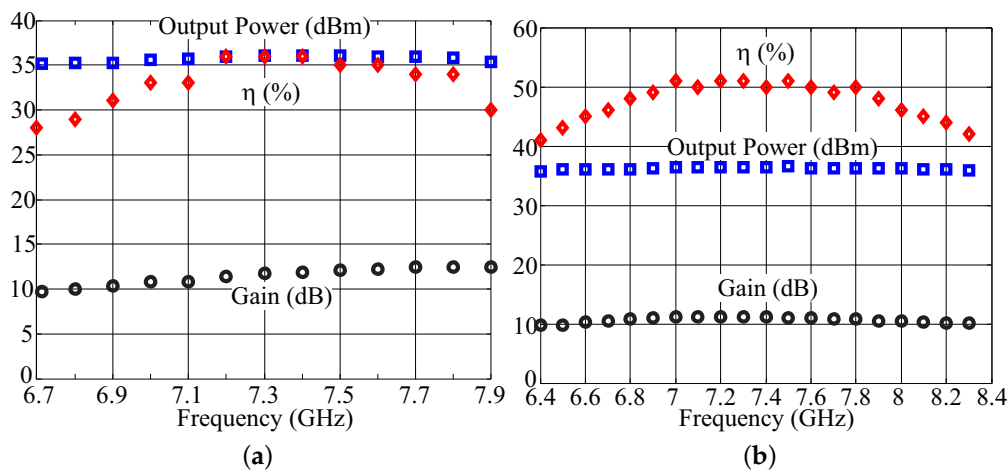


Figure 7. CW power performance *vs.* frequency for the Tuned Load (a), and Harmonic Tuned (b) PAs. Drain bias voltage is 30 V for both PAs. Drain bias current is 60 and 30 mA, respectively.

Table 1 compares the designed 7 GHz PAs (Tuned Load: TL, Harmonic Tuned: HT) with some GaAs commercial PAs, in terms of frequency, saturated output power and saturated efficiency. The performance in terms of output power and efficiency are similar, but the higher power density of GaN allows to reach the target power with only two devices of around 1 mm of periphery, while in both the commercial examples a 2/3 stages and a larger periphery are necessary. For example, in the TGA2701 the two stages PA employs in the final stage two branches of 2×8 devices (for a total of 20 devices including the 4 devices of the first stage). This higher complexity impacts on area, requires power dividers/combiners, has less advantageous impedance levels and limits the attainable power and efficiency. This demonstrates the possibility to adopt GaN as an alternative to GaAs for 7 GHz backhaul MMIC PAs.

Table 1. Comparison between the designed 7 GHz GaN PAs and commercial GaAs examples.

Ref.	Frequency (GHz)	P _{OUT} (dBm)	PAE (%)
HMC7357	5.5–8.5	35.5	35
TGA2701	7–8.5	37	42
TL	6.7–7.9	35	28
HT	6.4–8.3	36	42

2.2.2. System Level Characterization

The adopted system-level characterization set-up includes an arbitrary waveform generator (AWG) that generates the microwave modulated signal, a receiver based on a vector signal analyzer (VSA), and a workstation (PC) for the elaboration of the data. The input data stream is loaded into the AWG, modulated, up-converted and sent to the amplifier input. The VSA receives the output data stream, and computes after down-conversion and demodulation the required system level FoMs. The two PAs have been measured applying a 256-QAM, input signal with 7 MHz of channel and Peak to Average Power Ratio (PAPR) of 7.4 dB. The MMICs have then been modeled and predistorted with a memory polynomial model well adopted for its simplicity that makes it well suited to FPGA implementation. The linearity have been tested applying the simplest predistorter required to comply with a standard ETSI spectrum emission mask for a 7 MHz channel signal (the maximum affordable

with the available measurement setup) with raised-cosine filter, roll-off of 0.2, 256-QAM modulation and PAPR of 7.4 dB (see [15], p. 29, mask type 6L). The resulting spectra are shown in Figure 8.

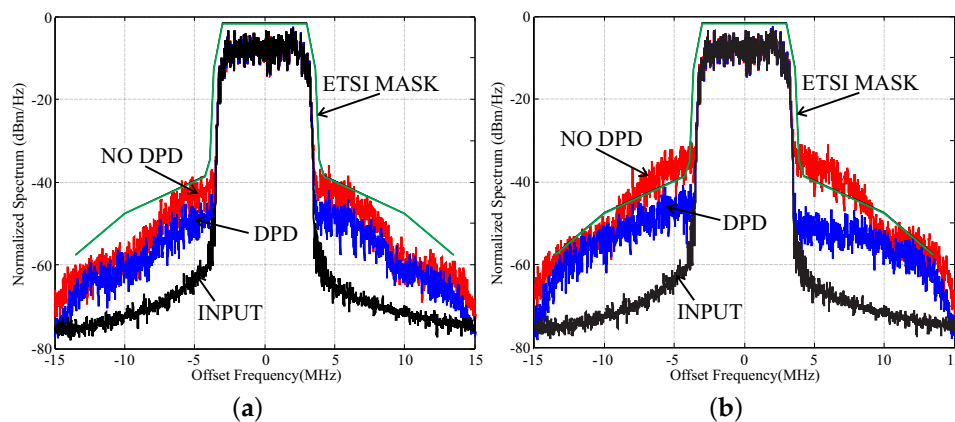


Figure 8. Normalized power spectra from system level measurements without (red) and with digital pre distorter (DPD) (blue, polynomial order 3, memory depth 0). Tuned Load amplifier (a), Harmonic Tuned amplifier (b). Applied baseband signal: 256-Quadrature Amplitude Modulation, 7 MHz channel, Peak to Average Power Ratio of 7.4 dB (black). For reference, ETSI 6L standard emission mask is reported in green.

To summarize these results we can say that the Harmonic Tuned stage clearly outperforms the Tuned Load under all the analyzed FoMs in CW conditions. However, the Tuned Load amplifier exhibits a more linear behaviour than the Harmonic Tuned, allowing for predistortion at power back-off equal equal to the PAPR of 7.4 dB (average output power of 28.4 dBm), with a simple scheme. For the Harmonic Tuned amplifier the same linearizer can be used, but an additional back-off of around 1 dB is required, hence partially reducing the advantages of this scheme in terms of average output power (same level of the Tuned Load amplifier 28.4 dBm). On the other hand, some advantages from the efficiency point of view can still be appreciated, with average efficiency in this case of 24%, instead of the former 18%.

3. Class AB PAs for 15 GHz Microwave Backhaul

While the use of 0.25 μm GaN technology for frequencies up to 10 GHz is well explored in the literature [16,17], and commercial products are already available, few examples can be found at higher frequencies. The design of the MMIC PA for 15 GHz backhaul has the aim to explore the capabilities of the adopted technology in Ku-band, to assess whether it can still be considered a viable alternative to GaAs solutions.

3.1. Design Strategy and Fabrication

The 15 GHz PA has been based on a combined topology, using class AB biased transistors. The output capacitance, due to the high frequency of operation, is assumed to provide low impedance at harmonics. As a consequence, the design of the output matching mainly consists on the synthesis of the optimum termination at fundamental for maximum output power. The complete schematic of the PA can be seen in Figure 9, where the transmission line electrical lengths refer to 15 GHz. Semi-lumped networks have been designed to provide a good compromise between losses and circuit size.

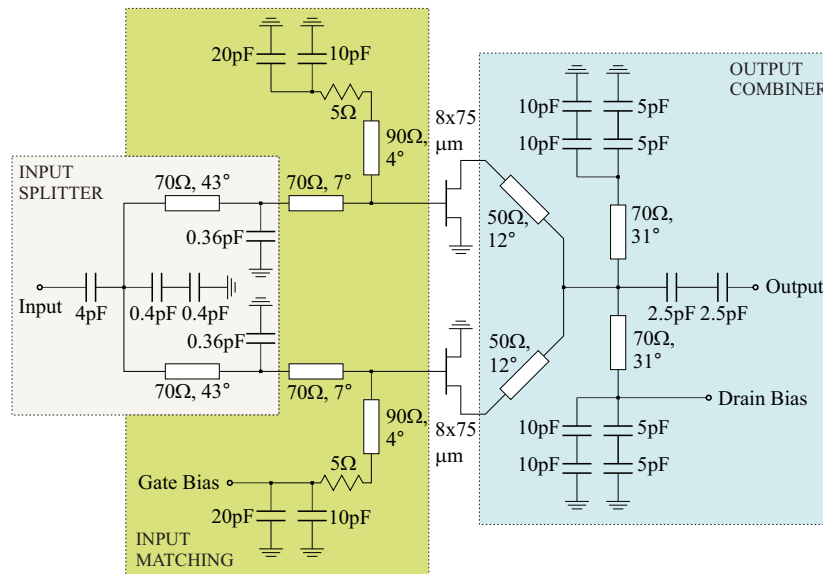


Figure 9. Complete scheme of the 15 GHz combined Amplifier. Equivalent ideal lines are represented: electrical length refers to 15 GHz.

The output combiner, the drain bias stub (actually splitted in two symmetrical stubs), and the decoupling capacitors are designed to provide output matching and to supply drain bias. Input matching and broadband stabilization are provided by a short stub on the gate side, with a series resistance of $5\ \Omega$, while large by-pass capacitors are used to guarantee good isolation also at low frequencies. The input power divider is a semi-lumped splitter. Since the needed input capacitance resulted to be very low, two larger series capacitors have been employed to improve the robustness of the circuit.

Figure 10 shows the microscope picture of the fabricated 15 GHz MMIC PA, whose size is $2.3 \times 1.3\ \text{mm}^2$.

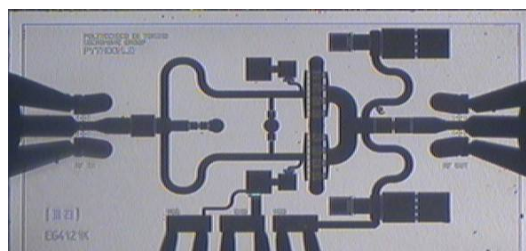


Figure 10. Microscope picture of the 15 GHz ($2.3 \times 1.3\ \text{mm}^2$) MMIC combined amplifier.

3.2. Experimental Characterization

The fabricated PA has been characterized in small signal in the band 12–18 GHz, in large signal in the band 14–16 GHz, and with a 256-QAM, 7 MHz channel modulated input signal for linearity assessment. The bias drain voltage has been set to 30 V, with a drain bias current of 30 mA.

3.2.1. Small signal and Continuous Wave

Figure 11 shows the measured scattering parameters, compared with the simulations, of the 15 GHz combined PA, with drain bias of 30 V, 30 mA, in the 12–18 GHz band. It can be seen that the gain is higher than 6 dB from 14 to 16 GHz.

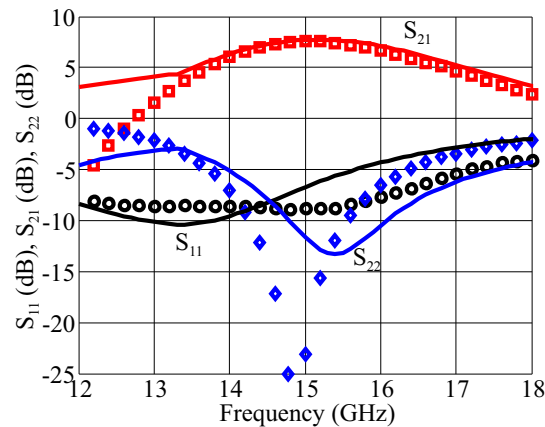


Figure 11. Scattering parameters in the band 12–18 GHz for the 15 GHz combined amplifier. Simulations: solid lines; measurements: symbols. S_{11} : black circles, S_{21} : red squares, S_{22} : blue diamonds.

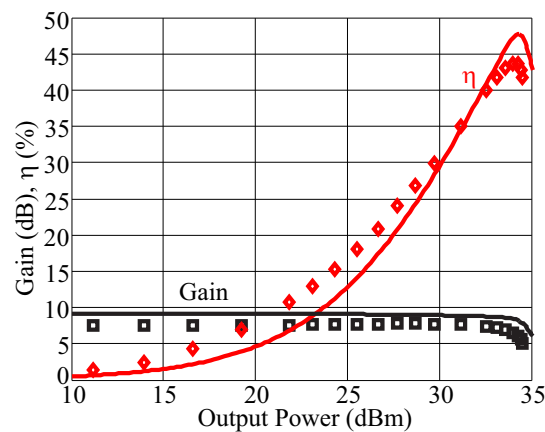


Figure 12. Power sweeps at 15 GHz of the class AB MMIC. Drain bias voltage and current are 30 V and 30 mA, respectively. Simulations: solid lines; measurements: symbols. Gain: black squares, efficiency: red diamonds.

Single tone characterization and simulation results at center frequency (see Figure 12), with drain bias of 30 V, 30 mA, show a saturated output power of 34.5 dBm, with corresponding efficiency of 42%, and small signal gain of 7.5 dB. With respect to the 7 GHz PA results, the output power results slightly lower, but a good efficiency can still be achieved.

Regarding the measured CW bandwidth, see Figure 13, the 15 GHz PA shows an almost constant saturated output power in the 14–16 GHz band, while the best saturated efficiency region is well-centered around 15 GHz, with values exceeding 40%. Table 2 compares the characterization results of the 15 GHz PA with the performance of commercially available GaAs PAs, with similar frequency band and output power.

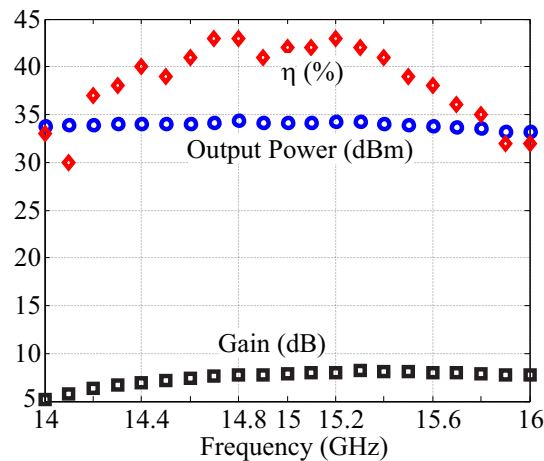


Figure 13. CW power performance *vs.* frequency for the amplifier. Drain bias voltage and current are 30 V and 30 mA, respectively. Measurements: symbols, simulations: solid lines.

Table 2. Comparison between the designed 15 GHz Gallium Nitride (GaN) PA and commercial gallium arsenide (GaAs) examples.

Ref.	Frequency (GHz)	P _{OUT} (dBm)	PAE (%)
HMC995	12–16	34.5	34
TGA2533	12.5–15.5	33.8	31
This PA	14–16	34	32

In addition, in this case, the advantages offered by GaN in terms of simplicity and area constraints, already pointed out in the previous example at lower frequency, are still present and even more evident. In fact, while output power and efficiency are still comparable with the commercial examples, the complexity is clearly different. Both the commercial examples employ 3/4 stages and in the TGA2533 the three stages PA requires in the two branches $2 \times 4 \times 8$ devices (for a total of 28 devices) with impact on size, cost, reliability. This confirms that, with the progressing of the GaN process maturity, GaN will most likely be a valid alternative to GaAs for backhaul PA applications.

3.2.2. System Level Characterization

Also for the 15 GHz PA, to prove the linearizability of the designed stage, system level measurements and predistortion have been performed. A test signal using a 256-QAM modulation with 7 MHz channel and PAPR of 7.4 dB has been applied. The linearity has been tested applying the simplest predistorter required to comply with a standard ETSI spectrum emission mask (see [15], p. 29, mask type 6L). As for the 7 GHz case, a memory polynomial predistorter has been adopted for its simplicity and effectiveness. Figure 14 shows the measured output spectra before and after predistortion, proving the linearizability of the designed MMIC and its compliance with the ETSI emission mask.

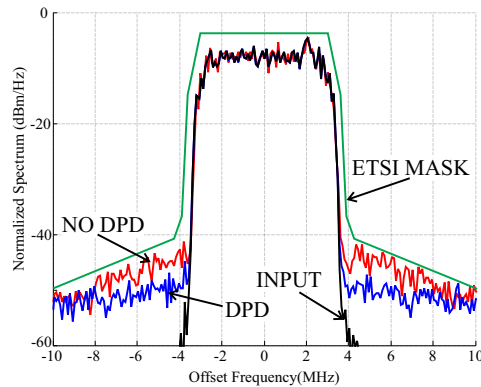


Figure 14. Normalized power spectra from system level measurements on the 15 GHz combined PA. Applied baseband signal: 256-QAM, 7 MHz channel, Peak to Average Power Ratio (PAPR) of 7.4 dB.

4. Conclusions

Three design examples of MMIC GaN power amplifiers for microwave backhaul applications have been shown. The capability of 0.25 μm GaN technology to enable the design of compact monolithic, efficient and linear power amplifiers for frequencies up to the Ku-band has been demonstrated. In fact, not only the measured large signal results exhibit good output power and efficiency, but also the linearizability of the proposed PAs with simple predistortion schemes, assessed through system level characterizations, has been proven to be feasible.

Acknowledgments: Ericsson AB is acknowledged for the support.

Author Contributions: Roberto Quaglia participated to the design of the circuits and to their characterization; he wrote the paper. Vittorio Camarchia participated to the design and to the characterization of the circuits, and wrote the article. Marco Pirola supervised the design and the characterization, and reviewed and corrected the paper. Giovanni Ghione reviewed and corrected the paper.

Conflicts of Interest: The authors declare no conflict of interest.

Abbreviations

The following abbreviations are used in this manuscript:

QAM	Quadrature Amplitude Modulation
AM	Amplitude Modulation
PM	Frequency Modulation
HEMT	High Electron Mobility Transistor
FoM	Figure of Merit
AM/AM	Amplitude to amplitude modulation distortion
AM/PM	Amplitude to phase modulation conversion
PAPR	Peak-to-Average Power Ratio
OBO	Output Back-Off

References

1. Kenington, P. *High Linearity RF Amplifier Design*; Artech House: Boston, MA, USA, 2000.
2. Camarchia, V.; Quaglia, R.; Pirola, M. Transmitter. In *Electronics for Microwave Backhaul*; Camarchia, V., Quaglia, R., Pirola, M., Eds.; Artech House: Boston, MA, USA, 2016; pp. 205–284.
3. Chia, S.; Gasparroni, M.; Brick, P. The next challenge for cellular networks: Backhaul. *IEEE Microw. Mag.* **2009**, *10*, 54–66.
4. Pengelly, R.S.; Wood, S.M.; Milligan, J.W.; Sheppard, S.T.; Pribble, W.L. A Review of GaN on SiC High Electron-Mobility Power Transistors and MMICs. *IEEE Trans. Microw. Theory Tech.* **2012**, *60*, 1764–1783.

5. Camarchia, V.; Donati Guerrieri, S.; Pirola, M.; Teppati, V.; Ferrero, A.; Ghione, G.; Peroni, M.; Romanini, P.; Lanzieri, C.; Lavanga, S.; *et al.* Fabrication and nonlinear characterization of GaN HEMTs on SiC and sapphire for high-power applications. *Int. J. RF Microw. Comput.-Aided Eng.* **2006**, *16*, 70–80.
6. Reveyrand, T.; Ciccognani, W.; Ghione, G.; Jardel, O.; Limiti, E.; Serino, A.; Camarchia, V.; Cappelluti, F.; Quéré, R. GaN transistor characterization and modeling activities performed within the frame of the KorriGaN project. *Int. J. Microw. Wirel. Technol.* **2010**, *2*, 51–61.
7. Camarchia, V.; Moreno Rubio, J.; Pirola, M.; Quaglia, R.; Colantonio, P.; Giannini, F.; Giofre, R.; Piazzon, L.; Emanuelsson, T.; Wegeland, T. High-Efficiency 7 GHz Doherty GaN MMIC Power Amplifiers for Microwave Backhaul Radio Links. *IEEE Trans. Electron Devices* **2013**, *60*, 3592–3595.
8. *TriQuint Semiconductor 0.25- μ m Gallium Nitride 3MI, Process Data Sheet*; TriQuint Semiconductor: Richardson, TX, USA, 2009.
9. Quaglia, R.; Camarchia, V.; Pirola, M.; Rubio, J.J.M.; Ghione, G. Linear GaN MMIC Combined Power Amplifiers for 7-GHz Microwave Backhaul. *IEEE Trans. Microw. Theory Tech.* **2014**, *62*, 2700–2710.
10. Dawson, D.E. Closed-form solutions for the design of optimum matching networks. *IEEE Trans. Microw. Theory Technol.* **2009**, *57*, 121–129.
11. Saad, P.; Fager, C.; Cao, H.; Zirath, H.; Andersson, K. Design of a Highly Efficient 2–4-GHz Octave Bandwidth GaN-HEMT Power Amplifier. *IEEE Trans. Microw. Theory Technol.* **2010**, *58*, 1677–1685.
12. Moreno Rubio, J.; Fang, J.; Camarchia, V.; Quaglia, R.; Pirola, M.; Ghione, G. 3–3.6 GHz wideband GaN Doherty power amplifier exploiting output compensation stages. *IEEE Trans. Microw. Theory Technol.* **2012**, *60*, 2543–2548.
13. Colantonio, P.; Giannini, F.; Limiti, E. *High Efficiency RF and Microwave Solid State Power Amplifiers*; Wiley: Hoboken, NJ, USA, 2009.
14. Camarchia, V.; Teppati, V.; Corbellini, S.; Pirola, M. Microwave Measurements -Part II Non-linear Measurements. *IEEE Instrum. Meas. Mag.* **2007**, *10*, 34–39.
15. ETSI EN 302 217-2-2. Fixed Radio Systems; Characteristics and requirements for point-to-point equipment and antennas; Part 2-2: Digital systems operating in frequency bands where frequency co-ordination is applied. Available online: http://www.etsi.org/deliver/etsi_en/302200_302299/3022170202/02.00.00_20/en_3022170202v020000c.pdf (accessed on 29 May 2016)
16. Gustafsson, D.; Chani Cahuana, J.; Kuylenstierna, D.; Angelov, I.; Rorsman, N.; Fager, C. A wideband and compact GaN MMIC Doherty amplifier for microwave link applications. *IEEE Trans. Microw. Theory Technol.* **2013**, *61*, 922–930.
17. Piotrowicz, S.; Ouarch, Z.; Chartier, E.; Aubry, R.; Callet, G.; Floriot, D.; Jacquet, J.C.; Jardel, O.; Morvan, E.; Reveyrand, T.; *et al.* 43 W, 52% PAE X-Band AlGaIn/GaN HEMTs MMIC Amplifiers. In Proceedings of the IEEE MTT-S International Microwave Symposium Digest, Anaheim, CA, USA, 23–28 May 2010; pp. 505–508.



© 2016 by the authors; licensee MDPI, Basel, Switzerland. This article is an open access article distributed under the terms and conditions of the Creative Commons Attribution (CC-BY) license (<http://creativecommons.org/licenses/by/4.0/>).